Long-Range Order and Ordering Kinetics in $CoPt_3$

H. BERG AND J. B. COHEN

The Co-Pt system is well suited for studies of order-disorder by field-ion microscopy. Because of this, and the fact that detailed information on ordering is available for only one $L1_2$ alloy (Cu_3Au), an extensive X-ray study was made of $CoPt_3$. Long-range order falls to lower values ($S \approx 0.64$) in this alloy than in Cu_3Au. There is a two-phase field near T_c (685°C) extending for about 20°C. The ordered phase has a smaller lattice parameter than the disordered phase close to T_c, but at room temperature the reverse is true. Ordering (when the domain size is large) follows Rothstein's kinetic theory, with an activation energy of 74.0(9) kcal per g-atom. Domain growth is similar to grain growth, with a time exponent of about 0.45 and an average activation energy of about 62 kcal per g-atom. The antiphase domain structure is isotropic, in contrast to Cu_3Au. There is little difference in atomic volume of cobalt and platinum in the ordered state as compared to the pure elements.

THE Pt-Co system exhibits complete solubility at high temperatures with at least two ordered phases occurring at low temperatures,[1] Fig. 1. A tetragonal superlattice, well known for its good magnetic properties, forms near the composition CoPt.[2] Near the composition $CoPt_3$, an $L1_2$-type superlattice (Cu_3Au) was first reported by Geisler and Martin.[3] They determined the critical temperature (T_c) for an alloy with 30 at. pct Co to lie between 700° to 800°C. However, a temperature of 630° to 650°C was reported by Menzinger and Paoletti[4] in a study, with neutron diffraction, on an alloy of 24.9 at. pct Co.

Detailed studies of ordering kinetics and order vs temperature are really only available for one alloy of the $L1_2$ type—namely Cu_3Au. Yet the Co-Pt alloys are widely employed in studies of ordering by field-ion microscopy.[5,6] This investigation was undertaken to provide such detailed information for proper heat treatment, to resolve the uncertainty in T_c, and to provide information on a superlattice isomorphous to Cu_3Au.

I) PROCEDURES

A) Specimens

The alloy was obtained from Engelhard Industries, Inc., as polycrystalline strip. Wet chemical analysis at several locations along the strip indicated a composition of 24.9 ± 0.15 at. pct Co; the principal impurities of Rh, Fe, Pd totaled less than 0.01 wt pct. Specimens employed for studies of lattice parameters and the kinetics of ordering and growth of antiphase domains were in the form of foils 7 mil thick. These were obtained by alternate rolling (to a reduction in thickness of nearly 100 pct) and annealing; the final reduction was 50 pct. The strip was then annealed at 725°C for 2 hr to produce a grain size of about 0.03 mm; this was done in the high-temperature attachment for the X-ray studies (see next section). The fine grain size was needed to minimize scatter in the measured X-ray intensities.

For studies of equilibrium order vs temperature, single crystals were grown from the strip by Metals Research Limited: a Bridgeman technique was employed under a pressure of inert gas to reduce vaporization of cobalt. Comparisons were made of the lattice parameters of annealed filings from the crystal and the strip; specimens were quenched from above T_c. From data reported by Gebhardt and Köster on lattice parameter vs composition,[7] the crystals were within 0.2 at. pct Co of the original strip. These crystals were then cut to expose a (100) face and polishing and repeated etching was continued until no further sharpening of Laue spots could be noted.

B) Equipment and Techniques

Lattice parameters of quenched powders were obtained with filtered CuK_α radiation and a camera of 114.6 mm diam. Values given are the result of a least-squares fit to peaks with $(h^2 + k^2 + l^2) = 16 - 24$, vs the

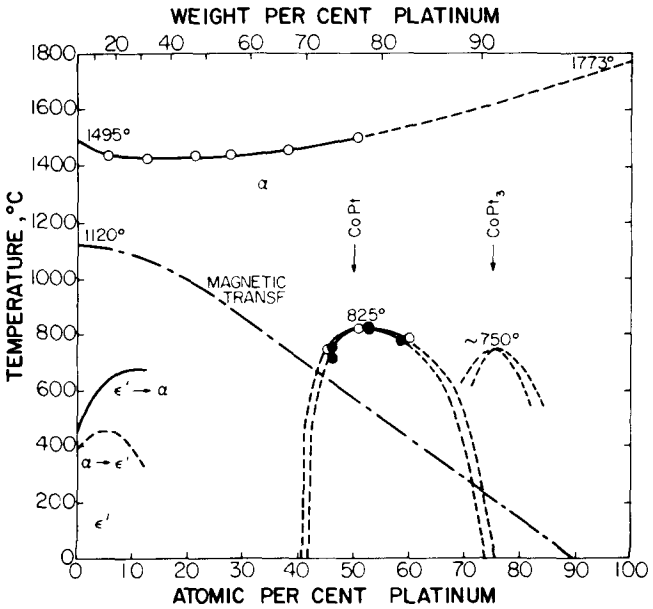

Fig. 1—Phase diagram for the Co-Pt system from Hansen.[1]

J. B. COHEN is Professor, Department of Materials Science, The Technological Institute, Northwestern University, Evanston, Illinois. H. BERG, Jr., formerly Research Assistant, Department of Materials Science, The Technological Institute, Northwestern University, is now with Motorola, Inc., Phoenix, Arizona. This paper is based upon a thesis submitted by H. BERG, Jr. in partial fulfillment of the requirements of the degree of Doctor of Philosophy at Northwestern University.

Manuscript submitted November 5, 1971.

Nelson-Riley parameter ($\frac{1}{2}\{\cos^2\theta/\sin\theta + \cos_2\theta/\theta\}$). All other studies were performed on G. E. XRD-5 Picker diffractometers, primarily at temperature (or in a vacuum of 10^{-5} torr or better) employing an MRC high-temperature attachment* or, where indicated, at room temperature. In the attachment, the specimen is heated by resistance; single crystals were spot-welded to platinum mesh for this purpose while for the foils, the heating element was the alloy foil itself. Two Chromel-Alumel thermocouples, 0.006 in. in diameter, were always attached to the specimen to measure temperature gradients and for control. These gradients were determined to be typically 3° to 5°C over the face of a specimen (0.3 in. by 0.35 in.) but the incident beam was generally reduced in size to keep the gradient to 1°C or less, especially in the vicinity of T_c. The temperature was controlled to ±0.5°C by a Thermac-Labac combination.*

*Materials Research Corporation, Orangeburg, New York.

*A silicon controlled rectifier and proportional control system manufactured by Radiation Instruments, Inc., Minneapolis, Minnesota.

The counting system consisted of a scintillation counter with a pulse height analyzer set to accept 90 pct of the K_α radiation. For measurements of peak depressions (due to thermal and static displacements from lattice sites) on specimens quenched from equilibrium at various temperatures, MoK_α was employed, monochromated with a doubly-bent LiF crystal in the incident beam. Otherwise filtered CuK_α was employed. All scans were made in the θ-2θ mode. For integrated intensities from single crystals (for measurement of equilibrium order at temperature or determination of peak depressions on quenched specimens), background was removed by averaging values on either side of a peak. Care was taken to open the receiving slits until the integrated intensity over background was constant. High-angle peaks were chosen to minimize extinction and to avoid rapid variations in background. The minimum net integrated intensity for a superstructure peak near T_c was of the order of 20,000 counts but was more typically 200,000 counts.

For studies of ordering and domain size vs time at various temperatures with the foil specimens, chart recordings were used unless otherwise noted. Goniometer speeds were chosen as slow as permissible but depended on the kinetics of the reaction at any temperature. Integrated intensities from chart recordings were obtained with a planimeter. Chart recordings were also employed to measure the width or position of a peak (from a single crystal or foil specimen) vs temperature after equilibrium was achieved.

Any heat treatment not performed in the high-temperature attachment was carried out in a vacuum of 10^{-5} torr or less with the specimen sealed in a quartz capsule. Resistance furnaces employed were controlled to ±3°C with gradients of 1°C over the length of the sample. Quenching, if required, was into ice water.

C) Diffraction Theory

The long-range order parameter (S) is defined in this study, following Cowley[8]

$$S = 3(r_\alpha - \tfrac{3}{4}) + \tfrac{1}{3}(r_\beta - \tfrac{1}{4}) \qquad [1]$$

where α represents A-atom sites and β represents B-atom sites in an A_3B, $L1_2$ alloy, r_i represents the fraction of sublattice i correctly occupied. Following Schwartz and Cohen,[9] the structure factor (F) has two forms for such an alloy. For fundamental peaks (hkl unmixed)

$$F_F = (3f_A + f_B)\ \exp\ [-(M_F^T + M'_F)] \qquad [2a]$$

For superstructure peaks (hkl mixed),

$$F_S = S|f_B - f_A|\ \exp[-(M_S^T + M'_S)] \qquad [2b]$$

where f_i is the atomic scattering factor of atom i, and the Debye-Waller factors are defined as follows:

$$M_F^T = [\tfrac{3}{4} - (\tfrac{3}{16})Sc]M_\alpha + [\tfrac{1}{4} + (\tfrac{3}{16})Sc]M_\beta \qquad [3a]$$

$$M_S^T = [\tfrac{1}{4} - 1/(Sc)]M_\alpha + [\tfrac{3}{4} + 1/(Sc)]M_\beta \qquad [3b]$$

[As long-range order disappears the two terms in Eq. [3b] blow up, but the structure factor also goes to zero. Furthermore, there are two terms of opposite sign in the equation.] Also: $c = 4(f_B - f_A)/(3f_A + f_B)$

$$M'_F = (\tfrac{3}{32})\epsilon^2\{Q_k(1 - S^2) + c(Q_k - 4Q_{1k})(S - 1)S^2/6\} \qquad [3c]$$

$$M'_S = (\tfrac{3}{32})\epsilon^2\{Q_k(1 - S^2) - \tfrac{4}{3}(Q_{1k} - Q_{2k})(S - 1)S - 8/(3c) \times (Q_{1k} + Q_{2k} - Q_{3k} - Q_{4k})(S - 1)\} \qquad [3d]$$

In these equations, $\epsilon = 1/4\pi(\omega_A - \omega_B)$ where the ω_i are the atomic volumes of the elements (not necessarily the volumes of the pure components). Also, M_F^T, M_S^T represent the contributions of mean-square thermal vibrations ($\langle\mu_T^2\rangle$) to the depression of Bragg peaks; the term $M_\alpha(M_\beta)$ has the form $8\pi^2\langle(\mu_T^\alpha)^2\rangle(\sin^2\theta/\lambda^2) = B_\alpha(\sin^2\theta/\lambda^2)$. The terms M'_F, M'_S represent the contributions due to mean-square static displacements from lattice sites. The terms in Q involve lattice sums and have been evaluated.[10]

$$Q_{1k} = 5.5k^2/a^4 \qquad [4a]$$

$$Q_{2k} = [11.7(k_1^2 + k_2^2) + 4.9k_3^2]/a^4 \qquad [4b]$$

$$Q_{3k} = [11.7(k_1^2 + k_3^2) + 4.9k_2^2]/a^4 \qquad [4c]$$

$$Q_{4k} = [11.7(k_2^2 + k_3^2) + 4.9k_1^2]/a^4 \qquad [4d]$$

and $Q_k = Q_{1k} + Q_{2k} + Q_{3k} + Q_{4k}$. $k_i = 2\pi h_i|\mathbf{b}_i|$ where $\mathbf{b}_i$ are the axes of the reciprocal lattice. Because of the $|k_i|$ terms in Q, the M' terms vary with $\sin^2\theta/\lambda^2$. Thus after measuring integrated intensities of fundamental peaks (P_F) and superstructure peaks (P_S), dividing by the Lorentz-polarization factor (LP) and utilizing Eq. [2],

$$\ln\left[\frac{1}{(3f_A + f_B)}\left(\frac{P_F}{\text{L.P.}}\right)^{1/2}\right] = \frac{1}{2}\ln K - (M_F^T + M'_F) \qquad [5a]$$

$$\ln\left[\frac{1}{S|f_B - f_A|}\left(\frac{P_S}{\text{L.P.}}\right)^{1/2}\right] = \frac{1}{2}\ln K - (M_S^T + M'_S) \qquad [5b]$$

Straight lines are obtained if the left sides of Eq. [5] are plotted vs $\sin^2\theta/\lambda^2$. The term K is just a proportionality constant between integrated intensity and F^2; it includes the direct beam's intensity, absorption, and so forth, and is independent of angle for a flat crystal cut for symmetrical diffraction and larger than the incident beam. The value of S is found that gives the same ordinate for Eqs. [5a] and [5b]. This treatment assumes that the vibrational amplitude of an atom depends only on the sublattice it occupies. For $S = 1$, there is no difference between this treatment and one which considers the vibration to depend on the atom

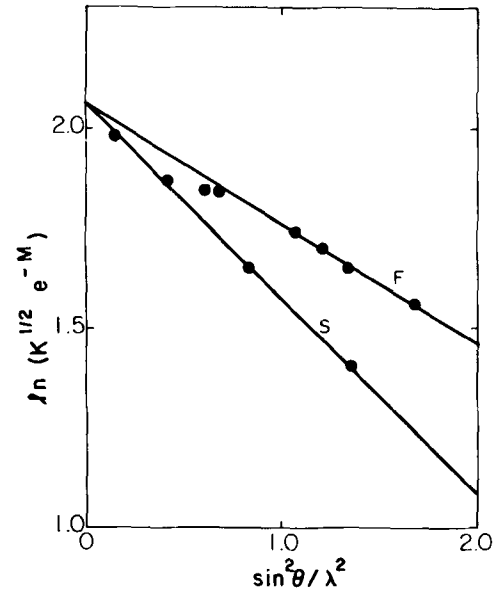

(a)

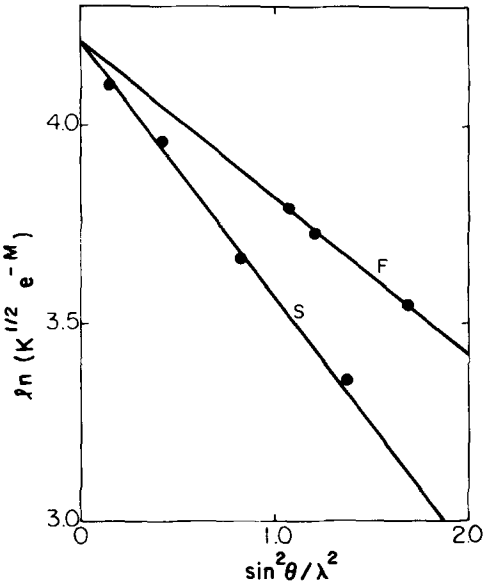

(b)

Fig. 2—$\ln K^{1/2}e^{-M}$ vs $\sin^2\theta/\lambda^2$ where $K^{1/2}e^{-M}$ is the square root of the integrated intensity divided by the L. P. factor and F^2. *S*, superstructure peaks (300, 500, 700, 900); *F*, fundamental peaks (600, 620, 800, 660, 840, 1000); measurements at T = 298 K. (*a*) Slow-cooled, S = 1.01; (*b*) quenched from 660°C, S = 0.73 (600, 620, and 840 peaks were not measured).

type; *i.e.* all A atoms are on the α sublattice and all B atoms are on the β sublattice. Also, for this case, the M' terms vanish and B_α^T, B_β^T can be determined. With these values, and for $S < 1$, ϵ can be determined.

This procedure was utilized at room temperature on single crystals equilibrated to give $S = 1$ and three other states of order (the heat treatments will be given with the results). Knowing M_α, M_β and M'_F, M'_S as a function of order, the ratio of the integrated intensities of the 300 and 400 peaks from a single crystal at any temperature was then employed to obtain S.

$$S = \left\{\frac{P_S}{P_F}\frac{(\mathrm{LP})_F}{(\mathrm{LP})_S}\right\}^{1/2}\frac{|3f_A + f_B|}{|f_B + f_A|}\frac{\exp[-(M_F^T + M'_F)]}{\exp[-(M_S^T + M'_S)]} \qquad [6]$$

The measured integrated intensities in Eqs. [5] and [6] contain unwanted contributions due to thermal-diffuse scattering which peaks near the Bragg reflections as does the so-called "Huang peak" due to mean-square static displacements. The latter has been shown to be unimportant[9] but the former was corrected for one-phonon processes in the studies with single crystals using a computer program developed by Walker and Chipman.[11] (Their XTDL 2 program was used which neglects the incident beam's divergence.) Corrections ranged from 1 to 14 pct depending on the peak; the results were insensitive to errors in the elastic constants and to the crystal's precise orientation. The elastic constants employed were interpolated between the values at 25°C for platinum[12] and fcc cobalt.[13] Changing these to values at temperature following the changes for platinum[1] resulted in a change in S of less than 0.001. Changing the direction normal to the diffraction vector to ⟨013⟩ from ⟨001⟩ caused a change in S of 0.005 pct. Corrections calculated at room temperature were therefore used in the data taken with single crystals at all temperatures.

Antiphase domain sizes (D) were calculated from the half-widths (β) of superstructure peaks (corrected for instrumental errors) using the Scherrer equation:

$$\beta_{hkl} = \frac{0.9\lambda}{D_{hkl}\cos\theta} \qquad [7a]$$

β was obtained from the actual half-widths (B) and the instrumental breadths for an infinite domain size (b). The latter value was obtained at the correct 2θ by extrapolating the breadths of fundamental peaks,

$$\beta = \{\sqrt{B^2 - b^2}\cdot(B - b)\}^{1/2} \qquad [7b]$$

This is an average value for Gaussian and Cauchy peak shapes and has been shown to give reasonable agreement with values obtained from transmission electron microscopy.[14]

II) RESULTS

A) Debye-Waller Factors

A $CoPt_3$ crystal (crystal 1) was initially heat treated as follows: 1 hr at 710°C, 24 hr at 670°C, 72 hr at 665°C, 72 hr at 655°C, 24 hr at 625°C, 24 hr at 600°C, 48 hr at 580°C, 48 hr at 550°C, 48 hr at 520°C, 120 hr at 500°C, 48 hr at 480°C, 48 hr at 460°C, 24 hr at 440°C, and air cooled. From the integrated intensities and Eq. [5], S = 1.01(3)* at 298 K. The error in S was estimated from least-mean-square fits of Eq. [5]. Another crystal (crystal 2) was ordered over a five month period; the integrated intensities resulted in S = 1.010 (25) from the data shown in Fig. 2(*a*). Two peaks on the line for the fundamentals were affected by extinction (they fall below the line) whereas no superstructure peaks were appreciably affected. Slopes for both fully ordered alloys yielded the rms vibrational amplitudes for platinum in Table I. Also presented are the Debye temperatures (θ_i) of platinum calculated from Eq. [8]:[15-17]

$$B_\alpha(T) = \frac{6h^2TN_A}{Mk\theta_\alpha^2}\left\{\varphi(\chi) + \frac{\chi}{4}\right\} \qquad [8]$$

*Values in parentheses indicate the standard deviation throughout the text.

Table I. Amplitudes of Thermal Vibration, Pt_3Co, $S = 1.01$ $T_{meas} = 298K$

		Crystal 1			Crystal 2		
Sublattice	Atom, γ	B_γ^T, Å^2	$\langle u_\gamma^2\rangle^{1/2}$, Å	θ_γ, K	B_γ^T, Å^2	$\langle u_\gamma^2\rangle^{1/2}$, Å	θ_γ, K
α	Pt	0.337	0.0653	229	0.331	0.0647	231
β	Co	−0.100			−0.086		

[Scattering factors and dispersion corrections were taken from D. T. Cromer and D. T. Mann, LASL Report LA-3689 (1967) and M. J. Copper, *Acta Cryst.*, 1963, vol. 16, p. 1067.]

Table II. Distortion Coefficient $|\epsilon|$ from Bragg Reflections for Pt_3Co (T = 298K for Measurement*)

S	B_F, Å^2	$\lvert\epsilon_F\rvert$, cm^3	B_S, Å^2	$\lvert\epsilon_s\rvert$, cm^3
0.87	0.340(24)	2.75×10^{-25}	0.568(21)	4.16×10^{-25}
0.855	0.331(24)	2.33×10^{-25}	0.585(20)	4.35×10^{-25}
0.835	0.338(13)	2.45×10^{-25}	0.587(21)	4.19×10^{-25}
0.73	0.388(24)	2.91×10^{-25}	0.626(24)	3.91×10^{-25}

*The following values were employed to obtain the listed values (from data on crystals with $S = 1.01$)

$$B_F^T = 0.297(17)\text{Å}^2$$

$$B_S^T = 0.479(17)\text{Å}^2$$

where h is Planck's constant, N_A is Avogadro's number, M is the atomic mass, k is Boltzmann's constant and $\chi = \theta_\alpha/T$. $\{\varphi(\chi) + (\chi/4)\}$ is a complex function of χ which was evaluated numerically by Zener.[15] The values in Table I can be compared to X-ray determinations for pure platinum at 25°C [236 (5) K].[17] The physically unreal negative term for B_β results because the α term dominates Eqs. [3a] and [3b]; the term in β is only a few percent of the terms in α. (See Ref. 18 for θ for pure cobalt.)

Four disordering treatments were performed by quenching specimens from 615°, 630°, 638°, and 660°C. (The quartz capsules did not shatter on quenching from 615° and 630°C so that these quenches were rather slow.) Values of S and peak depressions determined from the partially ordered alloys are given in Table II. The data after the quench from 660°C are shown in Fig. 2(b); the increases in the slopes due to static atomic displacements are clear. With the thermal amplitudes for the fully ordered alloy and the peak depressions for $S < 1.00$, it is possible to evaluate $|\epsilon|$, the difference in atomic volumes of platinum and cobalt from Eq. [3]. These values are also given in Table II. The average value of $|\epsilon|$ for all fundamental peaks is 2.61×10^{-25} cu cm and for all superstructure reflections is 4.15×10^{-25} cu cm. If platinum and cobalt maintain the radii of the pure elements $|\epsilon| = 3.1 \times 10^{-25}$ cu cm whereas data for a disordered (*i.e.* short range ordered) alloy indicates $\epsilon = 1.7 \times 10^{-25}$ cu cm.[19] Our values average to close to the former value. (Note also that the oscillations of the data points are the same in Figs. 2(a) and 2(b); these and other data suggdst that this is a real effect for which we as yet have no explanation.) In obtaining long-range order vs temperature (with Eq. [6]) in the next section, the temperature components B_F^T and B_S^T were assumed to vary with temperature according to Eq. [8], including a correction for the change in Debye temperature (θ_i) with volume:[20]

$$\frac{\theta(T)}{\theta(T_0)} = \left(\frac{a_0(T_0)}{a_0(T)}\right)^{3\gamma} \qquad [9]$$

where a_0 is the lattice parameter at the indicated temperature and γ the Gruneisen constant (the value was interpolated between values for cobalt and platinum).[21]

B) Long-Range Order

Initially a $CoPt_3$ crystal was subjected to the following ordering treatment: $\frac{1}{2}$ hr at 720°C, 72 hr at 670°C, 24 hr at 600°C, 24 hr at 550°C, 24 hr at 525°C, 48 hr at 500°C, 24 hr at 480°C, 24 hr at 470°C, 24 hr at 460°C, 24 hr at 450°C, 24 hr at 440°C, 24 hr at 430°C. The long-range order of this sample was determined from Eq. [6] to be 1.07 (1); the heat treatments for this alloy and the ones described in the previous section (for which $S = 1.01$) were similar, so the actual order is

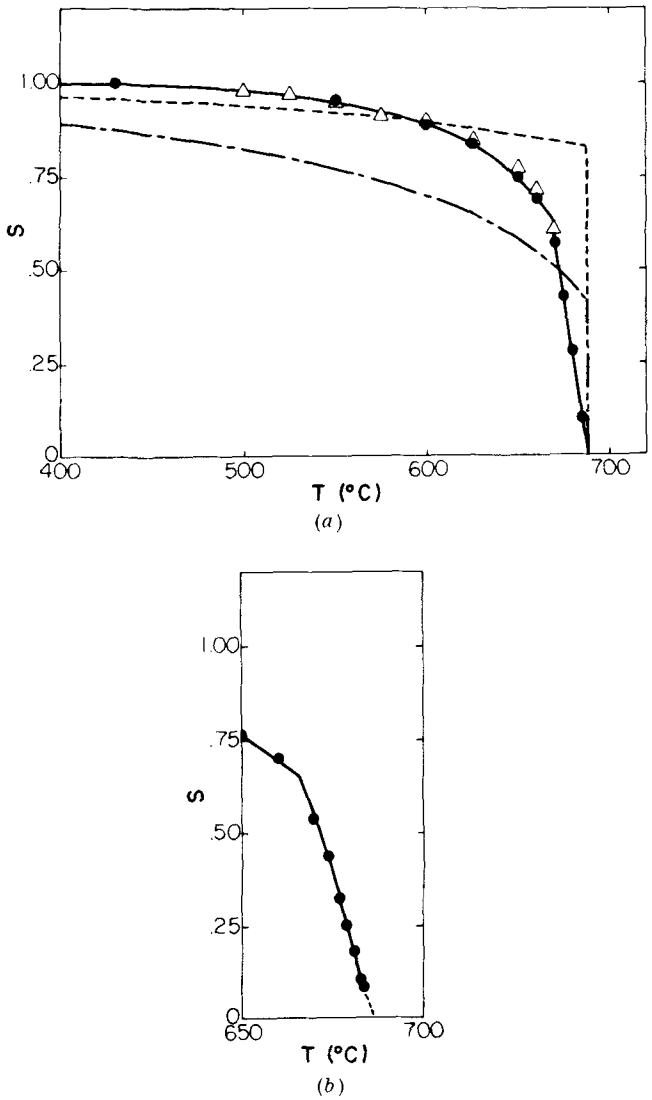

Fig. 3—(a) The normalized long-range order parameter as a function of temperature. Experimental results are given by the solid curve. The short-dashed curve gives the calculation by Cowley[8] and the long-dashed curve gives the calculation by Bragg and Williams.[22] Circles represent single crystal data whereas triangles represent data taken from polycrystalline foils. (b) Measurements of long-range order vs temperature near T_C using a smaller beam size than in (a).

likely close to unity (the higher value here is probably due to extinction in this crystal lowering the intensity of the fundamental peaks). For this reason, all values of S were normalized by dividing by 1.07. The crystal was then heated and held at various temperatures until the intensity of the 300 superstructure peak no longer decreased or until the data on ordering kinetics (section II. E) indicated that ordering was complete. Equilibrium long-range order vs temperature is presented in Fig. 3. S decreases continuously from 1 at 430°C to 0.64 at 668°C at which point it falls approximately linearly to zero. Included are data points from (at-temperature) measurements with a polycrystalline foil employing only the 100 peak, and assuming $S = 1.0$ at low temperatures.* The agreement is good. The ordering was found to be reversible from measurements taken on cooling as well as on heating. The predictions of the Cowley[8] and Bragg and Williams[22] theories for A_3B alloys are superimposed in the figure, showing that neither model describes this reaction properly.

*These data were corrected for the peak depression, but not for TDS, which is negligible at this position.

Evaluation of errors indicated that measuring statistics, use of interpolated elastic constants in the TDS correction and uncertainty in temperature (±1.5°C) result in errors in S of less than 0.01 at any temperature below 670°C. The main source of error is due to the uncertainties in the measured peak depressions. Employing standard deviations determined for B_F and B_S, the value of S measured at 430°C lies between 0.99 and 1.01, with 95 pct confidence limits; at 660°C, S lies between 0.72 and 0.76 with 95 pct confidence limits.

The linear decrease in S with temperature over the large interval of 20°C was bothersome. Since chemical analysis indicated a nearly stoichiometric composition, a sharper drop was expected. For this reason, the measurements above 650°C were repeated using a smaller beam size to further reduce gradients in temperature. More data points were included also near T_C. These data are plotted separately in Fig. 3 and indicate that the decrease in S with increasing temperature is not exactly linear between 668° to 685°C, but that the absolute slope increases slightly with temperature up to just below T_C. This is just the trend expected when passing through a two-phase region of ordered and disordered phases, if the fraction of the disordered phase increases nearly linearly with temperature while S of the ordered phase decreases (approximately) linearly with increasing temperature. The disordering kinetics were found to become sluggish near and above 670°C. Several days were required to reach "equilibrium" after temperature changes of only a few degrees in this region. This would be expected for nucleation and growth of a second phase. This possibility is considered further in the next section.

C) Broadening of Diffraction Peaks

Since the lattice parameters and compositions of ordered and disordered phases can be expected to differ in any two-phase region, the high-angle fundamental peaks should broaden (or split) if two phases are present near 670°C.

The breadth of the 400 peak at half height was measured from chart recordings between 650° and 700°C. As shown in Fig. 4 (circles) a slight broadening occurred between 668° to 684°C. Because this broadening was so small, an accurate step scanning motor with increments of 2 sec of arc was employed in another run to obtain the shape[23] (Δ's in Fig. 4). The slow disordering kinetics at 675°C allowed the broadening to be followed as a function of time over the several days required to reach equilibrium. The broadening is observed in the same temperature range as the approximately linear region of S vs T, further verifying the presence of two-phase region between 668° to 685°C. Unfortunately, the broadening was so slight that it was not possible to determine which side of the peak was broadened, so it is not known whether the ordered phase is platinum-rich or cobalt-rich.

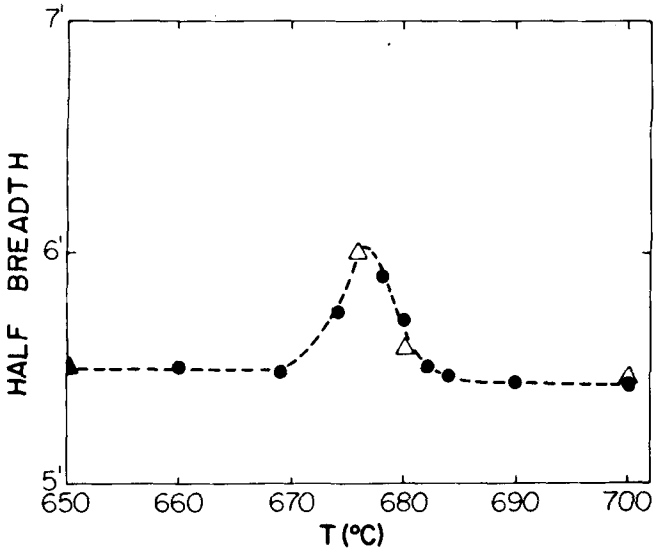

Fig. 4—Change with temperature of breadth at half height of the 400 reflection from $CoPt_3$. Circles represent data from chart recordings and triangles represent measurements employing step-scanning.

D) Lattice Parameters

The change in cell dimensions when Pt_3Co orders is another X-ray method of observing the ordering process, since the ordered phase generally has a more compact cell volume than the disordered phase. The position of the 420 peak vs temperature was utilized to examine the lattice parameter changes, as shown in Fig. 5. From this figure it is clear that lattice parameters of the ordered and disordered phases are most widely separated at high temperatures, rather than at room temperature, indicating different rates of thermal expansion (12.06 μin./in. °C and 12.66 μin./in. °C respectively). A continuous transition from the line of the ordered (or disordered) phase to the line of the other phase exists between 450° and 685°C. No discontinuous shift in peak position was observed at T_C and the maximum separation is only 6 min in 2θ. From this figure it can be seen that while the ordered phase has a smaller lattice parameter at temperature than the disordered phase, the latter appears to have a slightly smaller lattice parameter at room temperature. This finding is supported by lattice parameters from powder patterns of fully ordered and disordered Pt_3Co wires

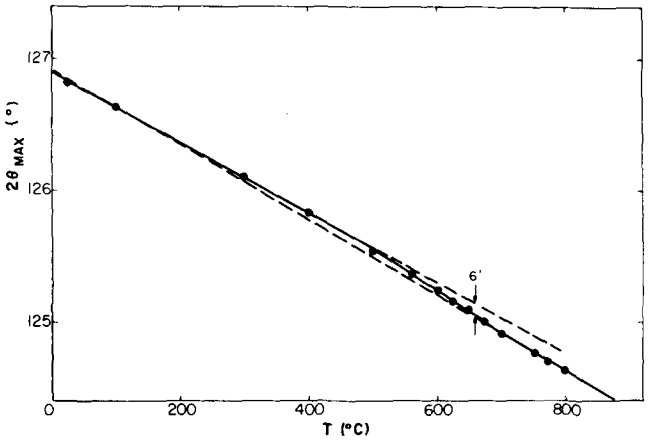

Fig. 5—Change with temperature of the position of the 420 reflection from $CoPt_3$. (Dashed lines are extrapolations.)

taken at room temperature (3.8539 (4)Å and 3.8530 (3)Å respectively for λ = 1.54051Å).

E) Kinetics of Ordering

If a partially ordered alloy with equilibrium long-range order and a large domain size is quenched from just below T_c to a lower temperature, the order within each domain will increase to the new equilibrium value with essentially no change in domain size. This homogeneous ordering process is to be distinguished from the nucleation and growth of domains operative in a specimen quenched from above T_c. The kinetics of this homogeneous ordering was studied by measuring the change in diffracted intensity of a superlattice peak over the time interval required to obtain the equilibrium value of S.

A polycrystalline foil, annealed for several days near 670°C to a domain size near 500Å, was quenched to the temperature of interest and the 100 peak was repeatedly scanned. Quenches were made from near 670°C to 625°, 600°, 575°, 550°, 525°, and 500°C. Typical experimental plots of S vs time after quench are given in Fig. 6 for T = 625° and 500°C. (The data were not corrected for TDS or peak depression. These corrections were negligible, primarily due to the low diffraction angle of the 100 peak, and the fact that a narrow range of integration was employed.) Ordering was complete in less than 50 min at 625°C while requiring several days at 500°C. Scatter in the data taken at higher temperature is considerably greater because of the fast scan rates required to record many peaks in a short time, compared to lower temperatures.

These data are summarized in the form of a time-temperature-transformation (TTT) diagram in Fig. 7. Curves corresponding to different percentages of completion of the reaction have been drawn, including data points at 670° to 675°C obtained from the investigations of the long-range order vs temperature. The noses of the curves are close to 665°C, although the kinetics do not become sluggish until nearly 670°C, where the two-phase region is encountered.

The most satisfactory approach to describing the kinetics of homogeneous ordering appears to be Dienes' chemical rate theory[24] in which the interchange of an A atom and a B atom from right sites of the stoichiometric superlattice to wrong sites is treated as a chemical reaction. The basic kinetic equation of the Dienes model is:

$$\frac{dS}{dt} = k_w \left\{ x_A x_B (1-S)^2 - \frac{\nu_r}{\nu_w} \left[S + x_A x_B (1-S)^2 \right] \times \exp\left[(-W/kT) \right] \right\} \qquad [10a]$$

where W is the Bragg-Williams energy ($W_0 S$), ν_r (ν_w) is the frequency for the interchange of right (wrong) atom pairs and k_w is the rate constant for the backward reaction. Because W depends on S, Eq. [10a] is trans-

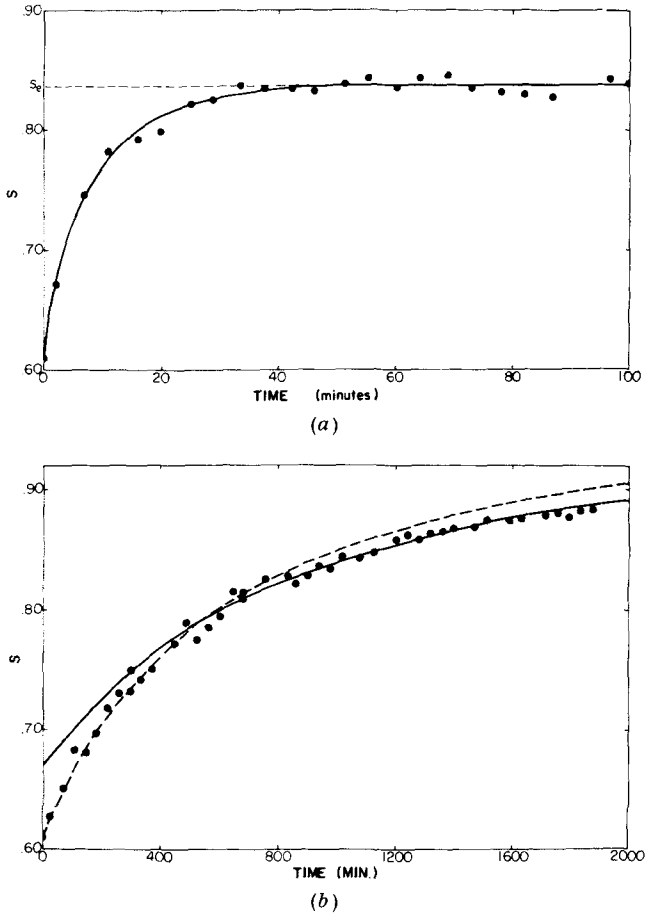

Fig. 6—Change in order with time after quench from 670°C. (*a*) T = 625°C; solid line is best overall fit with Eq. [10b]. (*b*) T = 500°C; solid line is fit with equation at long times; dashed line is fit at short times.

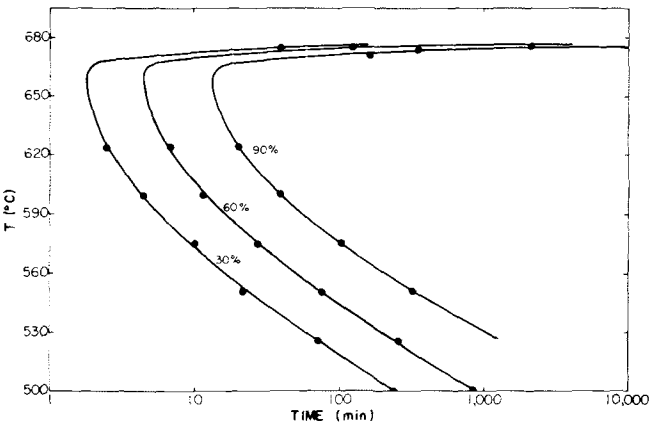

Fig. 7—Time-Temperature-Transformation diagram for ordering in $CoPt_3$.

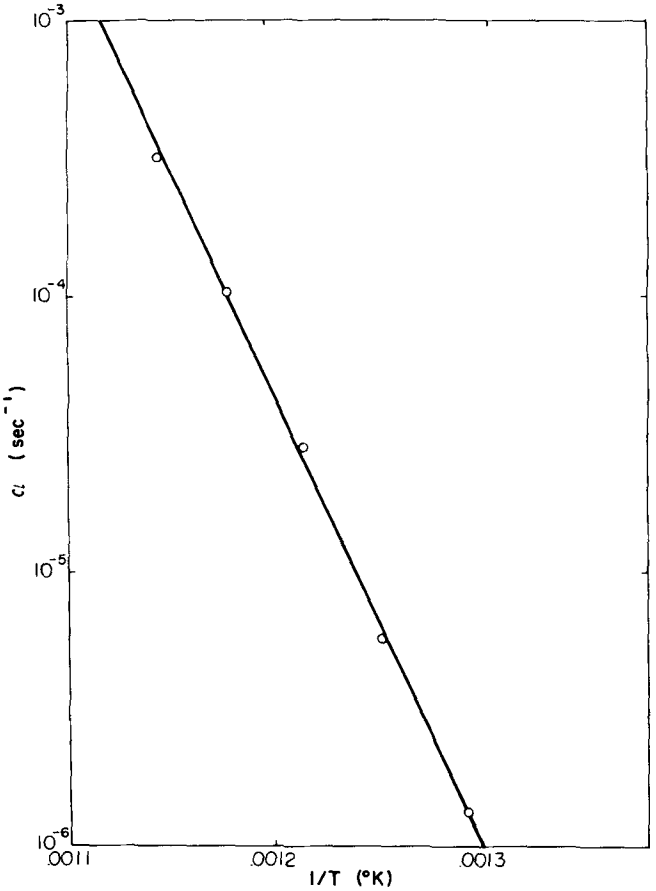

Fig. 8—The rate constant α in Eq. [11] as a function of the reciprocal absolute temperature.

cendental and may only be solved numerically for assumed values of the parameters. Nowick and Weisberg[25] have solved Eq. [10a] by a Taylor's expansion about the equilibrium long-range order, S_e, for small deviations from S_e. They showed that the resulting equation closely approximates the following expression developed earlier by Rothstein[26] under more restrictive conditions.

$$\left(\frac{1-S}{1-S_e}\right) = \begin{pmatrix}\coth\\ \tanh\end{pmatrix}(\alpha t + \beta) \qquad [10b]$$

where α is a complex function of S, W and the derivatives of W with respect to S; β is an integration constant. The tanh function applies to disordering. Rothstein's equation has been tested and been shown to fit the available data for small changes of long-range order in Cu_3Au.[27]

Eq. [10b] has been fitted to the latter part of each curve of S vs time for $CoPt_3$, thereby obtaining α and β as a function of temperature. At all temperatures the curve generated using α and β fits the experimental curve quite well except for short times after the quench, *e.g.* Fig. 6(*b*). This deviation at short times is expected since, in most cases, the total change in order is too large for the Nowick and Weisberg approximation to be strictly valid. (The change in order with time is greatest just after the quench where the fit with theory can then be expected to be worst.) Nowick and Weisberg show that to a good first approximation, α is given by

$$\alpha = (\nu_\gamma \nu_w)^{1/2}(x_A x_B)^{1/2}(Z_B/x_B) \times \exp\left[-\left(\left(\Delta H_{AB} + \tfrac{1}{2}W_0\right)/kT\right)\right] \qquad [11]$$

where Z_B is the number of B sites adjacent to an A site and ΔH_{AB} is the activation energy for the atomic interchange of a wrong A-B pair. The activation energy $(\Delta H_{AB} + \frac{1}{2}W_0)$ determined from the slope of a plot of ln α vs $1/T$, Fig. 8, employing a least-mean-square fit, is 74.0 (9) kcal per g-atom. The intercept yields a frequency factor, $(\nu_\gamma \nu_w)^{1/2}$, of 1.27×10^{14} sec^{-1}. If Eq. [11] is instead fitted to the initial part of each ordering curve, *e.g.* Fig. 6(*b*), the activation energy is 73.3 (12) kcal per g-atom with a frequency factor of 9.7×10^{13} sec^{-1}.

The activation energy determined from Fig. 8 appears to be larger than typical activation energies for diffusion controlled processes in alloys. Schoijet and Girifalco[27] have suggested that the activation energy determined in ordering experiments corresponds to the largest activation energy for a jump which increases S. For $CoPt_3$, the movement of a platinum atom from the cobalt to a platinum sublattice is the rate controlling step. This then should determine the activation energy or ordering, larger than what is measured in a diffusion experiment.

F) Growth of Antiphase Domains

In the completely ordered state, $CoPt_3$ has an $L1_2$ structure in which any one of the four sublattices can be occupied by cobalt atoms while the other three sublattices are occupied by platinum. The four possible unit cells are crystallographically related by shifts of $a/2\ \langle 110\rangle$. On quenching from above to below T_c, ordering occurs by a nucleation and growth process, because as we have shown the reaction is first order. Each ordered region is based on one of the four types of unit cell and grows by consuming the surrounding disordered material until regions impinge at "antiphase domain boundaries" (APDB). After impingement, some domains grow with the reduction in antiphase domain boundary area providing the driving force for growth. Simultaneously with the growth of ordered domains, the order within the domains may be in increasing.

In highly ordered Cu_3Au, the APDB have been found to lie primarily on $\{100\}$ planes.[28-30] Two types of APDB can occur on $\{100\}$ planes in an $L1_2$ alloy. One type has a low surface energy and is referred to as Type I [the shift of $a/2\ \langle 110\rangle$ lies *in* the (100) boundary]. The $\{100\}$ Type II APDB has nearest neighbor violations across the boundary making it a high energy boundary (the shift of $a/2\ \langle 110\rangle$ is perpendicular to the boundary plane). Also shear type APDB on $\{111\}$ planes can be produced by motion of a normal fcc dislocation with Burger's vector $a/2\ \langle 110\rangle$ through the ordered structure. From analyses proposed by Wilson[30] and Mikkola and Cohen,[31] the probability of $\{111\}$ shear, $\{100\}$ Type I and $\{100\}$ Type II APDB can be determined from the broadening of several superstructure peaks. In Cu_3Au the $\{100\}$ Type I APDB predominate at short times, with $\{111\}$ shear APDB increasing in importance at longer times. The $\{100\}$ Type I boundaries are quite evident in the diffraction pattern since these produce no broadening of 100 peaks but an abnormally large broadening of 110 peaks. For the other two types of boundary, both peaks are broadened but the 100 is broadened more than the 110.

A polycrystalline foil of $CoPt_3$ quenched from 700°C

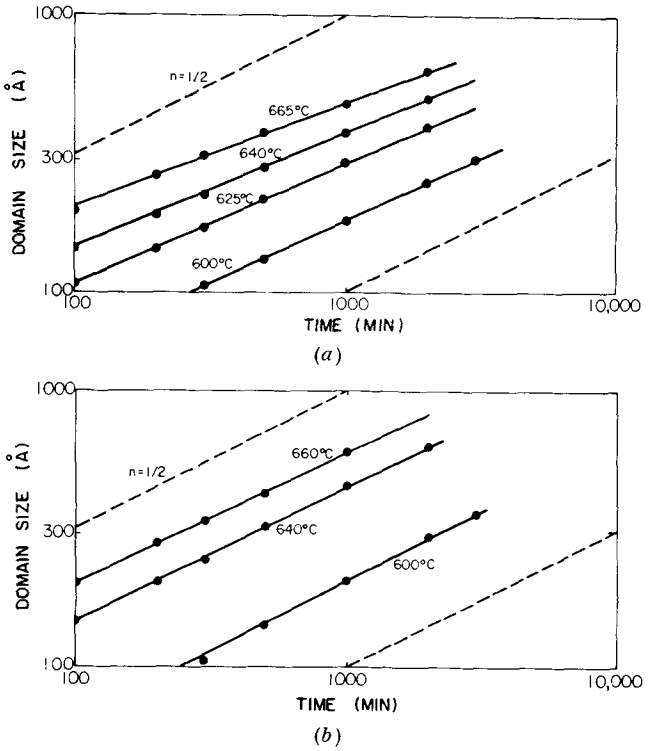

Fig. 9—Change in antiphase domain size with time after quench for various temperatures. (*a*) Domain sizes measured from broadening of 100 superlattice peak; (*b*) domain sizes obtained from 110 superlattice peak.

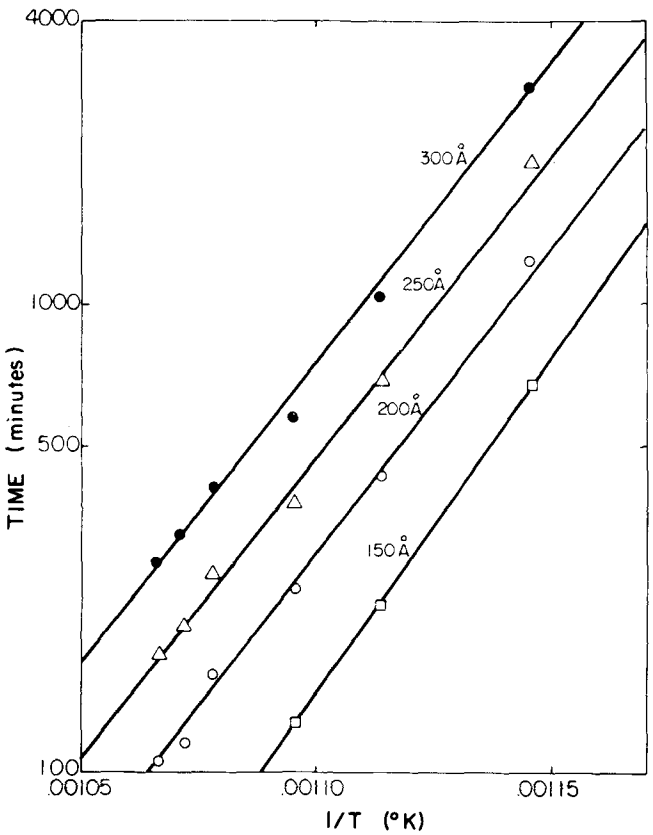

Fig. 10—Time to reach a given domain size vs reciprocal temperature (as measured from broadening of the 100 superlattice reflection).

was isothermally annealed below T_c for several days. The 100 and 110 superlattice peaks were examined many times, while the 210 and 211 peaks were examined only occasionally.

Broadening of the 211 superlattice peak after long annealing times (2 to 3 days) resulted in domain sizes similar to the 110, whereas the 210 reflection indicated slightly larger domain sizes than both the 110 and 211. Domain sizes obtained from the 100 and 110 peaks are similar at short annealing times with the 110 domain size increasing at a faster rate.

It is apparent that the APDB takes a more random orientation in $CoPt_3$ than in Cu_3Au.

Domain sizes were determined as a function of time for several quenching temperatures. It has been suggested by Rudman[32] that antiphase domain growth is analogous to grain growth and should follow the kinetic law:

$$D = kt^n + A \qquad [12]$$

where k and n are constants and t is the time. In Fig. 9, log D vs log t is plotted for the 100 and 110 peaks. All plots are linear with n varying between 0.38 and 0.45 for the 100 peaks and about 0.5 for the 110 reflection. (For metallurgical grain growth $n = 0.5$ is the predicted limiting value for high purity metals near the melting point, but experimental values range from 0.25 to 0.33.) Average activation energies of 63 kcal per g-atom and 61 kcal per g-atom were obtained from ln t vs reciprocal temperature at constant domain size for the 100 and 110 peaks, Fig. 10. Poquette and Mikkola[29] found that for Cu_3Au, $n \cong 0.5$ and that the activation energy obtained from studies of domain growth is the same as that found for diffusion in the alloy, indicating that domain growth is diffusion controlled. No diffusion data are available for the Pt-Co system, but activation energies determined from self diffusion of platinum (68 kcal per g-atom)[31] and cobalt (65 kcal per g-atom)[32] suggest the same is true in $CoPt_3$.

III) DISCUSSION AND SUMMARY

This research establishes that the order-disorder transformation in $CoPt_3$ is first order, as expected, but reveals the presence of a two-phase region between 668° to 685°C. That a significant two-phase region is present so close to stoichiometry is unusual when compared to other known superlattices. Also noteworthy is that Geisler and Martin[3] found the critical ordering temperature to be higher than 700°C for a 30 at. pct alloy as compared to 685°C in this investigation and to below 650°C in Menzinger and Paoletti's work.[4] A difference of 35°C in T_c determined by Menzinger and Paoletti and ourselves on nearly stoichiometric crystals suggests that T_c may vary sharply with composition near stoichiometry.

A relatively low degree of long-range order ($S = 0.64$) can be tolerated by $CoPt_3$ before disordering with a further increase in temperature, Fig. 3. In Cu_3Au the minimum degree of order is 0.80. This behavior for $CoPt_3$ may be partially due to the abnormally small difference in lattice parameters of the ordered and disordered phases. In Cu_3Au the difference in lattice parameters near T_c is 0.006Å as compared to 0.001Å in $CoPt_3$; significant changes in S in the former alloy result in larger strain energies.

The kinetics of ordering for $CoPt_3$ were found to fit Rothstein's[26] equation for ordering. An activation en-

ergy of 74 kcal per g-atom was found for the ordering process, which is probably associated with the motion of a platinum atom from the cobalt to the platinum sublattice. The kinetics of antiphase domain growth obey the equation describing grain growth, with an average activation energy of 62 kcal per g-atom. The broadening of superlattice peaks indicates that the low energy {100} Type I APDB are not as predominant for $CoPt_3$ as they are for Cu_3Au; a more random distribution of APDB is present.

Finally, we have noted that a partially ordered specimen is magnetic near 0°C, but a fully ordered specimen or a disordered specimen is not. This suggests more cobalt-rich regions in the first case than in the last, but a detailed study of local atomic arrangements in both cases would be interesting.

ACKNOWLEDGMENTS

This research was sponsored by the National Science Foundation. Support by a NDEA fellowship and by a Cabell fellowship from Northwestern University, are gratefully acknowledged. Drs. Walker and Chipman kindly made available their program for calculating TDS.

REFERENCES

1. M. Hansen: *Constitution of Binary Alloys,* 2nd ed., p. 493, McGraw-Hill Book Co., New York, 1958.
2. J. B. Newkirk, A. H. Geisler, D. L. Martin, and R. Smoluchowski: *AIME Trans.*, 1950, vol. 188, pp. 1249-60.
3. A. H. Geisler and D. L. Martin: *J. Appl. Phys.*, 1952, vol. 23, p. 375.
4. F. Menzinger and A. Paoletti: *Phys. Rev.*, 1966, vol. 143, pp. 365-72.
5. T. T. Tsong and E. W. Müller: *J. Appl. Phys.*, 1967, vol. 38, pp. 3531-36.
6. H. N. Southworth and B. Ralph: *Phil. Mag.*, 1970, vol. 21, pp. 23-41.
7. E. Gebhardt and W. Köster: *Z. Metallk.*, 1940, vol. 32, pp. 253-61.
8. J. M. Cowley: *Phys. Rev.*, 1950, vol. 77, pp. 669-75.
9. L. H. Schwartz and J. B. Cohen: *J. Appl. Phys.*, 1965, vol. 36, pp. 598-616.
10. A. A. Smirnov, E. A. Tikhonova, and A. V. Chalyi: *Sov. Phys. Solid State,* 1962, vol. 4, pp. 55-59.
11. C. B. Walker and D. R. Chipman: *Acta Cryst.*, 1970, vol. A26, pp. 447-55.
12. R. E. Macfarlane, J. A. Rayne, and C. K. Jones: *Phys. Lett.*, 1965, vol. 18, pp. 91-92.
13. R. D. Dragsdorf: *J. Appl. Phys.*, 1960, vol. 31, pp. 434-36.
14. D. E. Mikkola and J. B. Cohen: *Acta Met.*, 1966, vol. 14, pp. 105-22.
15. C. Zener: *Phys. Rev.*, 1936, vol. 49, pp. 122-37.
16. R. W. James: *The Optical Principles of the Diffraction of X-rays,* pp. 218-20, G. Bell and Sons, Ltd., London, 1954.
17. K. Alexopoulous, J. Boskouitis, S. Mourikis, and M. Roilos: *Acta Cryst.*, 1965, vol. 19, pp. 349-53.
18. R. Lagnegorg and R. Kaplow: *Acta Met.*, 1967, vol. 15, pp. 13-24.
19. P. S. Rudman and B. L. Averbach: *Acta Met.*, 1957, vol. 5, pp. 65-73.
20. A. Paskin: *Acta Cryst.*, 1957, vol. 10, pp. 667-69.
21. J. C. Slater: *Phys. Rev.*, 1940, vol. 57, pp. 744-46.
22. W. L. Bragg and E. J. Williams: *Proc. Roy. Soc.*, 1934, vol. A145, pp. 699-730; 1935, vol. A151, pp. 540-66.
23. J. B. Cohen, R. Dixon, M. Hayakawa, and L. Morrison: *Rev. Sci. Inst.*, 1969, vol. 40, p. 1235.
24. G. J. Dienes: *Acta Met.*, 1955, vol. 3, pp. 549-57.
25. A. J. Nowick and L. R. Weisberg: *Acta Met.*, 1958, vol. 6, pp. 260-65.
26. J. Rothstein: *Phys. Rev.*, 1954, vol. 94, p. 1429.
27. M. Schoijet and L. A. Girifalco: *J. Phys. Chem. Solids,* 1968, vol. 29, pp. 911-22.
28. F. W. Jones and C. Sykes: *Proc. Roy. Soc.*, 1938, vol. A166, pp. 376-90.
29. G. E. Poquette and D. E. Mikkola: *Trans. TMS-AIME,* 1969, vol. 245, pp. 743-51.
30. A. J. C. Wilson: *Proc. Roy. Soc.*, 1943, vol. A181, pp. 360-68.
31. D. E. Mikkola and J. B. Cohen: *Local Atomic Arrangements Studied by X-ray Diffraction,* pp. 289-337, Gordon and Breach, New York, 1966.
32. C. J. Smithells: *Metals Reference Handbook,* p. 644, Plenum Press, New York, 1967.
33. P. S. Rudman: *Intermetallic Compounds,* p. 405, J. H. Westbrook, ed., J. Wiley and Sons, New York, 1966.